Supporting Information

Strained calcite crystals from amorphous calcium carbonate containing an organic molecule

So Sugiyama, Mihiro Takasaki, Yuya Oaki, and Hiroaki Imai*

Department of Applied Chemistry, Faculty of Science and Technology, Keio University, 3-14-1 Hiyoshi, Kohoku-ku, Yokohama 223-8522, Japan.   E-mail*: hiroaki@applc.keio.ac.jp
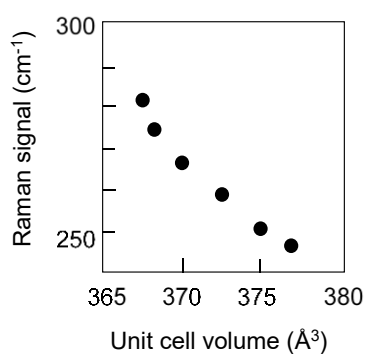
Fig. S1 Relationship between the cell volume and the Raman scattering signal at 280 cm^{-1} of calcite. This graph was reproduced from data that were presented in Ref #1.

Experimental section

(a) Synthesis of amorphous calcium carbonate

We mixed 2.0 cm^3 alkali solutions of 0.1 mol/dm^3 Na$_2$CO$_3$ and 0.1 mol/dm^3 CaCl$_2$•2H$_2$O at pH 12 with cooling to 0 °C with iced water. The pH value was adjusted by addition of an NaOH solution. Certain amounts of aspartic acid (Asp, Asp/Ca = 0–30mol%) were dissolved in the calcium solution before mixing. White precipitates that were immediately obtained in the mixtures were removed by suction filtration for 1 min with a membrane filter from the mother solution. We washed the precipitates with dehydrated acetone and subsequent suction filtration for 1 min. Finally, amorphous calcium carbonate (ACC) containing Asp was obtained by drying of the precipitates at 120 °C for 12 h in a vacuum oven.
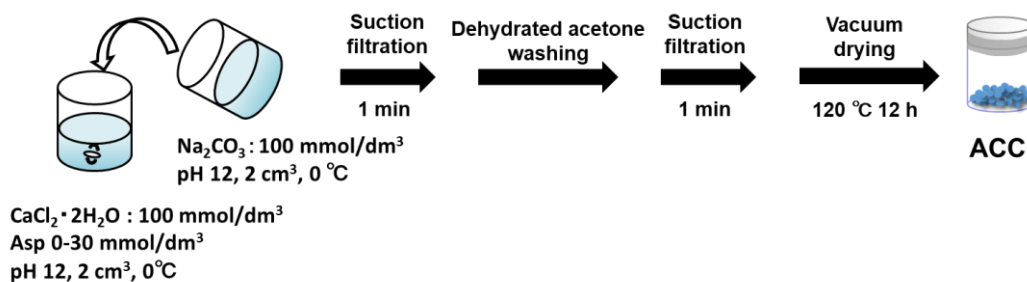
Fig. S2 Schematic illustration for the production of ACC nanoparticles.

(b) Structural characterization

We characterized the morphological evolution and the crystalline phase of $CaCO_3$ in the dispersion with scanning electron microscopy (SEM, JEOL JSM-7100F, operated at 5.0 kV), transmission electron microscopy (TEM, FEI Tecnai G^2, operated at 200 kV) with selective area electron diffraction (SAED), X-ray diffraction (XRD, Bruker D8 Advance Eco, operated at 40 kV and 25 mA), and Raman scattering microscopy (Renishaw inVia with a 532 nm laser as an excitation light). The spectral resolution of the Raman scattering spectrometer is 1 cm^{-1}. Thus, the variation of the Raman signals that was observed in the present manuscript is outside the resolution. The dispersion was dropped on a copper grid covered with a collodion film for TEM observation. The contents of Asp and water in ACC nanoparticles were estimated by the weight loss in air on TG using a Seiko TG/DTA7200 thermal analyzer.

(c) Evaluation of mechanical properties

We prepared pellets 13 mm diameter and 0.2–0.3 mm thick with the white powder of 50 mg in a mold by an oil press with 370 MPa. The pellets before and after calcination were embedded in a resin and then polished with waterproof abrasive paper (#1500) to evaluate the mechanical properties by a microhardness tester (Shimadzu DUH-211S) using the Berkovich-type indenter with a ridge angle of 115°. We obtained hardness (H) and Young modulus (E) from loading-unloading curves (25 mN, n = 15) using the Oliver–Pharr method.
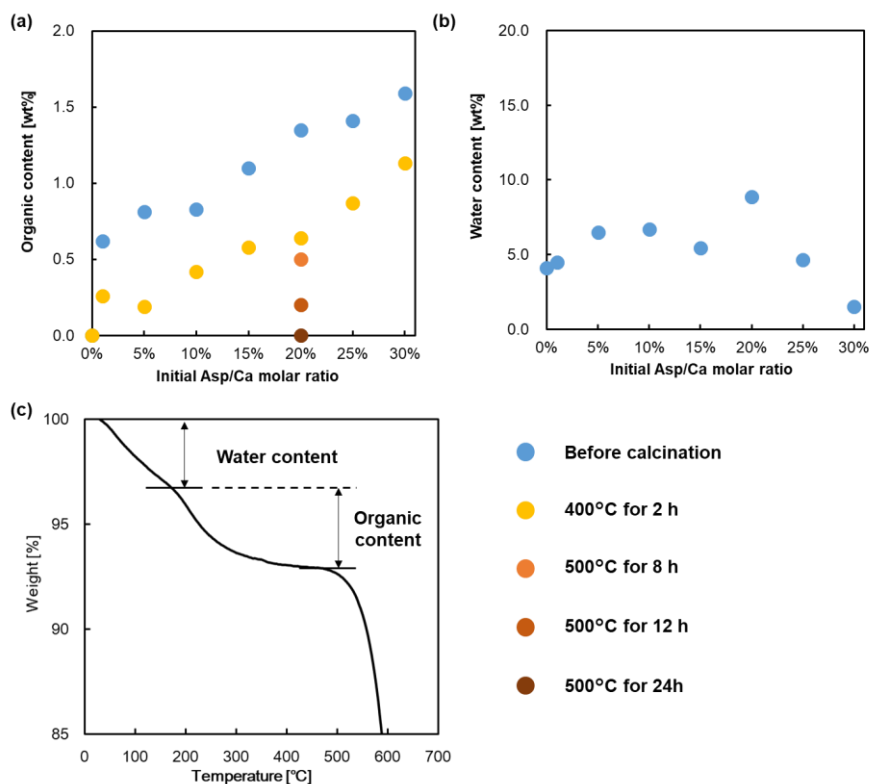
Fig. S3 The contents of organic molecules (a) and water (b) estimated from TG curves for ACC and calcite nanoparticles as a function of the initial concentration of Asp in the precursor solution. A typical TG curve for ACC nanoparticles obtained in the mother solution containing 10mol% Asp is shown in (c).
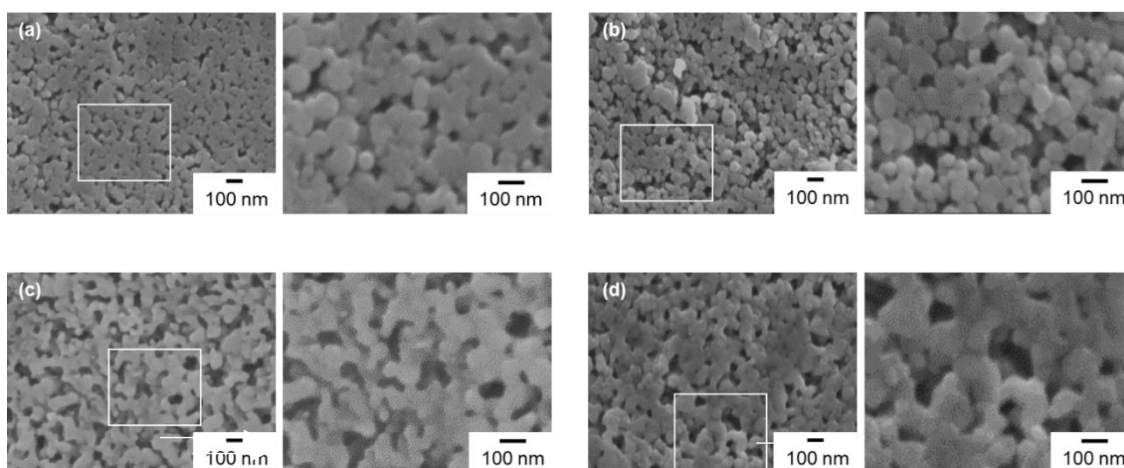

Fig. S4 SEM images of nanoparticles before (a, b) and after calcination (c, d) at 400°C for 2 h. The initial content of Asp in the mother solution: (a, c) 0% and (b, d) 10mol%.
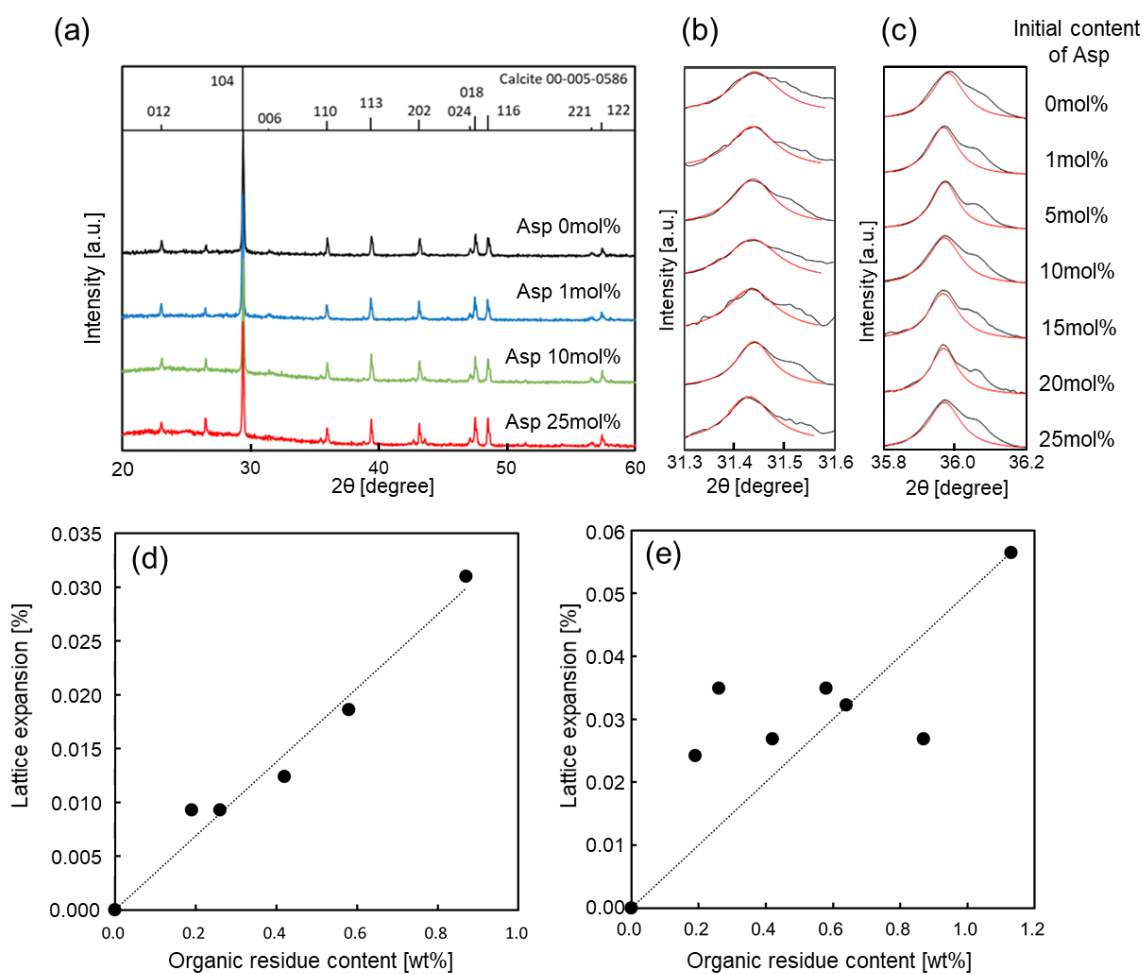
Fig. S5 XRD patterns of nanoparticles after calcination at 400 °C for 2 h (a). The lattice expansion of the *c* (d) and *a* (e) axes evaluated from the shift of 006 (b) and 110 (c) signals, respectively. The X-ray diffraction signal around 27° suggests the presence of aragonite or vaterite as an impurity phase. Unfortunately, an accurate judgment was not made because other characteristic signals were not observed in the diffraction patterns due to its low content.
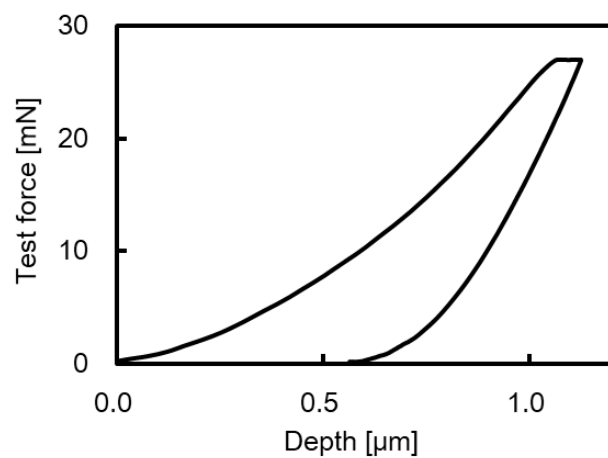
Fig. S6 Typical loading and unloading curves of the indentation test for calcined nanoparticles.
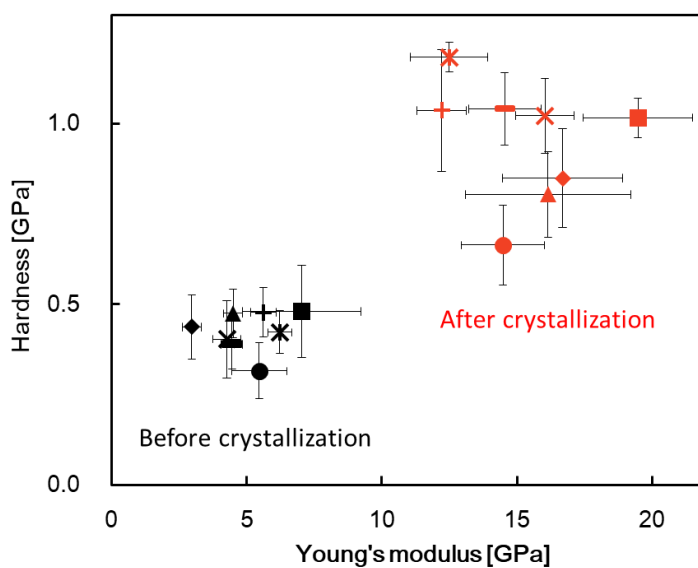

Fig. S7 Hardness (*H*) and Young's modulus (*E*) of pellets of ACC nanoparticles before and after calcination at 400 °C for 2 h. The initial content of Asp in the mother solution: ● 0, ▲ 1, ◆ 5, ■ 10, × 15, * 20, − 25, + 30mol%.
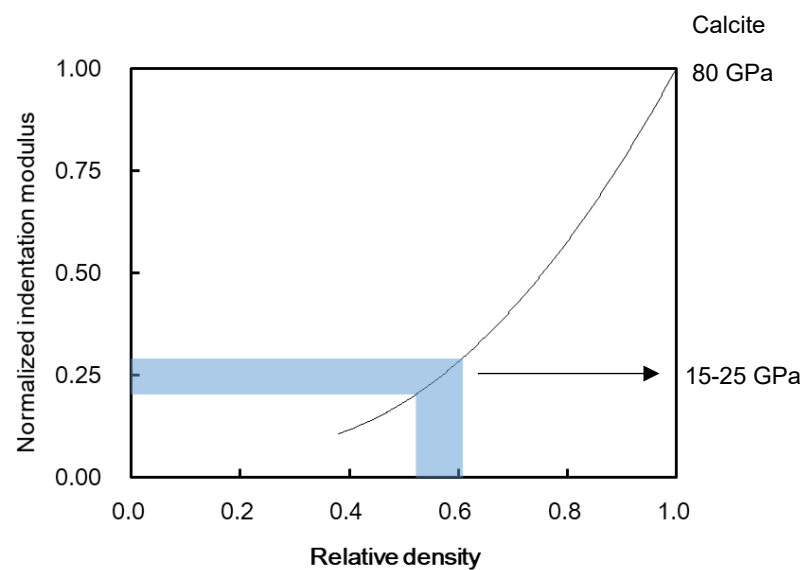
Fig. S8 Normalized modulus of porous silica as a function of relative density.[2]

References

1. P. Gillet, C. Biellmann, B. Reynard, P. McMillan, *Phys. Chem. Minerals*, 1993, **20**, 1–18.

2. D. Jauffrès, C. Yacou, M. Verdier, R. Dendievel and A. Ayral, *Microporous Mesoporous Mater.*, 2011, **140**, 120–129.